THEORETICAL INVESTIGATION OF HEAT AND MASS TRANSFER FOR HOLLOW FIBRE INTEGRATED EVAPORATIVE COOLING SYSTEM

Xiangjie Chen[1], Yuehong Su[1], Saffa Riffat[1], Amir Amini[2], Zhengxu Wang[3]
.
*Author for correspondence
[1]Department of Architecture and Built Environment, University of Nottingham, United Kingdom, NG7 2RD
[2]Spirax Sarco Ltd, Charlton House, Cheltenham, GL53 8ER, United Kingdom
[3]School of International Relations and Public Affairs, Fudan University, China,200433
E-mail: xiangjie.chen@nottingham.ac.uk

ABSTRACT

Due to the advantages of light weight, corrosive resistant and low cost, hollow fibres have been studied as the substitute for metallic materials. A novel hollow fibre integrated evaporative cooling system, in which the hollow fibre module constitutes as the humidifier and evaporative cooler, is proposed. This novel hollow fibre integrated evaporative cooling system will provide a comfortable indoor environment for hot and dry area. Moreover, the water vapour can permeate through the hollow fibre effectively, and the liquid water droplets will be prevented from mixing with the processed air. A mathematical model, which takes into account of the heat transfer between incoming air and the circulating water inside the fiber, and the water evaporation through the fibre, is developed and analyzed. The variations of incoming air velocity, fibre inside diameter, the incoming air temperature and humidity on the evaporative cooling effectiveness were discussed in this paper. The results showed that as the incoming air velocity increased from 0.2m/s to 0.8m/s, the saturation efficiency was between 0.52 and 0.84. The theoretical investigation revealed that this novel hollow integrated evaporative cooling system is compact, which offers relatively high heat and mass transfer performance.

INTRODUCTION

As the global warming effect continues to pose threats on the world climate, more and more countries start to rely on air conditioning systems to provide indoor thermal comfort during summer season. In the global scale, the conventional vapour compression system is the most widely used system for air conditioning purpose. However, it is driven by electricity which not only consumes a lot of primary energy but also associated with very high carbon emission. Attempts have been made to employ systems which consume less energy with lower carbon emissions. This is where the evaporative cooling system comes into place.

Direct evaporative cooler, is a simple design where direct contact is made between ambient air to be cooled, and the water. The interaction between air and water results in evaporation of a small amount of water, while the latent heat of evaporation causes simultaneous reduction in the air temperatures. This process is based on the conversion of sensible heat into latent heat. Sensible heat is heat associated with a change in temperature. While changes in sensible heat affect temperature, it does not change the physical state of water. Conversely, latent heat transfer only changes the physical state of a substance by evaporation or condensation[1].As water evaporates, it changes from liquid to vapour. This change of phase requires latent heat to be absorbed from the surrounding air and the remaining liquid water. As a result, the air temperature decreases and the relative humidity increases. The maximum cooling that can be achieved is a reduction in air temperature to the wetbulb temperature[2].

Evaporative cooling technologies have been extensively studied by researchers, with focus on pad incorporated evaporative cooling system[3-6], desiccant based evaporative cooling system[7], and dew point based evaporative cooling system[8-11]. Among this, porous pad incorporated evaporative cooling system is the most simplest type due to the fact that the porous packing materials in the cooling chamber provide very large contact surface for the mixing of the water and incoming air flows, while at the same time ensuring that the transfer process take place with as little time as possible. A number of studies have been carried out to better understand the performance of wetted media. ANSI and ASABE [12]recommended the air speeds and minimum water flows for aspen fiber and corrugated cellulose media. Franco [13] studied the influence of water and air flows on the performance of cellulose media. Dowdy et al. [14] experimentally determined the heat and mass transfer coefficients in aspen media and rigid impregnated cellulose media.

Different from traditional paper based evaporative cooling system, a novel hollow fibre integrated evaporative cooling system is proposed in this paper. With the micro size diameter of the hollow fibre (OD<0.1mm), the contact surface area between the air and cooling water is significantly increased. Moreover, by varying the porosity and the fibre inside and outside diameter, the cooling effect of the evaporative system could be adjusted accordingly. Most importantly, the fibre materials are generally made from PP, PVDF or PPS, which are cheap to produce, environmental friendly, and flexible for recycling. These advantages makes the hollow fibre integrated evaporative cooling system a promising substitute for conventional vapour compression system. This paper theoretically studied the heat and mass transfer process for the hollow fibre integrated evaporative cooling system. The effects of the fibre inside/outside diameter, fibre length and incoming air speed on the air saturation efficiency, heat and mass transfer coefficients and the amount of evaporated water are analysed numerically.

Figure 2 Hollow fibre bundles (provided by ZENA Ltd.)

NOMENCLATURE

A	[m2]	*Heat transfer area*
Cp	[J/Kg K]	Specific heat
h	[KJ/Kg]	enthalpy
k	[W/mK]	Thermal conductivity
L	[m]	Length
$\dot{m}$	[kg/s]	Mass flow rate
T	[K]	Temperature
Nu	[-]	Nusselt number
Pr	[-]	Prandtle number
Q	[W]	Heat transfer rate
Re	[-]	Reynolds number
U	[W/m²K]	Overall heat transfer coefficient

Special characters

ρ	[kg/m3]	Density
η	[-]	Saturation efficiency

Subscripts

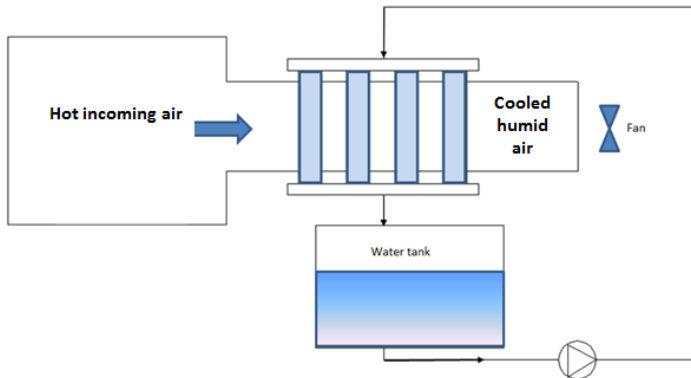|	
H	Heat transfer
M	Mass transfer
s	Shell side
t	Tube side
wb	Wet bulb
v	vapour

MATHEMATICAL MODEL

Figure 1 Schematic diagram of the polymer hollow fibre integrated evaporative cooling system

This paper analyses the heat and mass transfer process of the polymer hollow fibre integrated evaporative cooling system. As shown in Figure 1, hot incoming air, with temperature in the range of 35-40°C and humidity of 30-50%, will pass through a circular duct. The polymer hollow fibres (as shown in Figure 2), with ID=450μm and OD=550 μm will be formed into a bundle, which is fixed inside the circular duct. Cold water (temperature in the range of 10-15°C) will be circulated through the hollow fibre bundle with the help of a Centrifugal pump. When the hot incoming air get in contact with the hollow fibres, the water will be evaporated which leads to a decrease in temperature and increase in the humidity content of the air.

The basic heat and mass transfer equation:

$$q = m_a C_{pa}(T_1 - T_2) + m_a[\omega_1(h_{v1} - h_{wb}) - \omega_2(h_{v2} - h_{wb})]$$
Eq.(1)

$$m_e = m_a(\omega_2 - \omega_1)$$ Eq.(2)

Where q is the flow of transferred heat (W) ;

m_e is the flow of evaporated water(kg/h);

C_{pa} is the specific heat of dry air (KJ/Kg K);

T_1 is the dry temperature of the incoming air (°C);

T_2 is the dry temperature of the outcoming air (°C);

h_{v1} and h_{v2} are the enthalpy of saturated water vapour at the entrance and exit of the hollow fibre circular duct (KJ/Kg);

h_{wb} is the enthalpy of saturated water vapour at the wet bulb temperature of the incoming air (KJ/Kg);

m_a is the mass flow rate of the incoming air (Kg/h);

The flow of transferred heat (q) and the flow of evaporated water (m_e) could be expressed as the product of heat transfer coefficient and the mean logarithmic difference in temperature (ΔT), and the product of the mass transfer coefficient and the mean logarithmic difference in the water vapour density (Δρ_V). These can be expressed in the following two equations:

$$q = h_H A_s \, \Delta T$$ Eq.(3)
$$m_e = h_M A_s \Delta\rho_V$$ Eq.(4)

Where h_H is the coefficient of heat transfer (W/m2K);

h_M is the coefficient of mass transfer (W/m2K);

A_s is the total surface area of the hollow fibre (m2);

The mean logarithmic difference in temperature (ΔT) and water vapour density (Δρ_V) can be calculated using following equations:

$$\Delta T = \frac{(T_2 - T_1)}{\ln(\frac{T_2 - T_{wb}}{T_1 - T_{wb}})}$$ Eq.(5)

$$\Delta\rho_V = \frac{(\rho_{V2} - \rho_{V1})}{\ln(\frac{\rho_{V1} - \rho_{wb}}{\rho_{V2} - \rho_{wb}})}$$ Eq.(6)

Where ρ_{V1} and ρ_{V2} are the water vapour density on entering and leaving the hollow fibres (kg/m³);

ρ_{wb} is the saturated water vapour density at the wet buld temperature (kg/m^3).

The heat and mass transfer coefficients could be expressed as:

$$h_H = \frac{Nu*k}{L} \qquad \text{Eq.(7)}$$

$$h_M = \frac{Sh*D_{AB}}{L} \qquad \text{Eq.(8)}$$

Where k is the thermal conductivity of the water (W/mK);

L is the characteristic length of the hollow fiber bundle.

The relationship between Reynolds number (Re) , Prandtl number (Pr) and Nusselt number (Nu), and the relationship between Reynolds number (Re), Schimidt number (Sc)and Sherwood number (Sh) can be expressed by:

$$Nu = C1Re^{m1}Pr^{1/3} \qquad \text{Eq.(9)}$$

$$Sh = C2Re^{m2}Sc^{1/3} \qquad \text{Eq.(10)}$$

Where C1,C2, m1, m2 are constants for the hollow fibre bundles.

The saturation efficiency (η) is an important expression used to characterise the air saturation capacity of the polymer hollow fibre bundle. This is defined as the ratio between the thermal difference on passing through the hollow fibre bundle ($T_1 - T_2$) and the maximum thermal difference that would occur if the air were saturated ($T_1 - T_{wb}$):

$$\eta = \frac{T_1 - T_2}{T_1 - T_{wb}} \qquad \text{Eq.(11)}$$

The amount of water evaporated from the hollow fibre bundle can be expressed as the mass flow of evaporated water per unit of exposed surface (A_f) and the thermal difference that can be achieved for given air conditions on entering the materials:

$$C_w = \frac{m_e}{(T_1 - T_2)A_f} \qquad \text{Eq.(12)}$$

SIMULATION RESULTS AND DISCUSSION

1.1 Air saturation efficiency

Figure 3 presents the variations of saturation efficiency with respect to various air velocities at different hollow fibre outside diameters (Do=375 μm, 575 μm, 775 μm, 975μm respectively). It can be found that the saturation efficiency decreases as the air velocities increases from 0.2m/s to 0.8m/s. For instance, considering the fibre outside diameter of 575 μm, as the air velocity reduces from 0.7m/s to 0.6m/s, the saturation efficiency increases from 0.58 to 0.65, with percentage increase of 12.1%. The reason is because as the air speed increase, the length of time which the air gets in contact with the water decreases, so does the saturation of the air, and consequentially the saturation efficiency is lower.

It is noteworthy that in order to achieve the same saturation efficiency, the required air speed will decrease as the fibre outside diameter increases. For example, in order to achieve the saturation efficiency of 0.7, the incoming air velocities should be 0.58m/s, 0.41m/s, 0.29m/s and 0.23m/s respectively for the hollow fibre outside diameters of 375μm, 575 μm, 775 μm and 975 μm. In another words, at larger fibre diameter, it would be easy to achieve higher saturation efficiency at lower air speed.
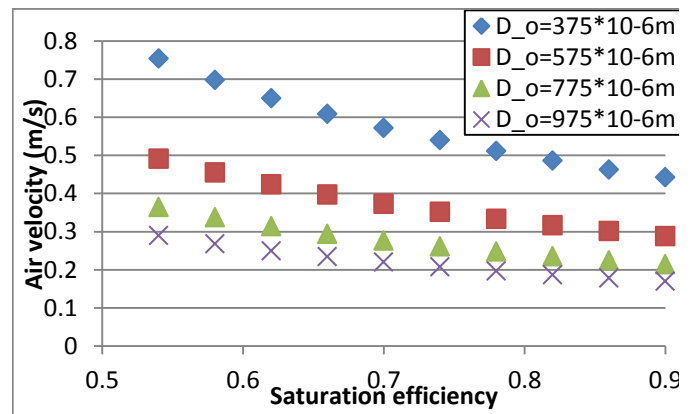
Figure 3 Variations of saturation efficiency with respect to various air velocities at different hollow fibre outside diameters
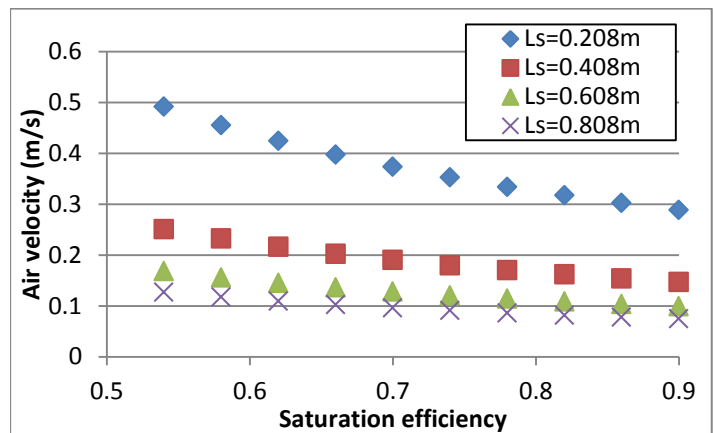
Figure 4 Variations of saturation efficiency with respect to various air velocities at different hollow fibre lengths

The variations of saturation efficiency with respect to various air velocities at different hollow fibre lengths (0.208m, 0.408m, 0.608m and 0.808m respectively) are depicted in Figure 4. It can be found that the saturation efficiency decreases as the air velocities increases from 0.2m/s to 0.5m/s. For instance, considering the fibre length of 0.408m, as the air velocity reduces from 0.25m/s to 0.15m/s, the saturation efficiency increases from 0.53 to 0.85, with percentage increase of 61.2%. Similar to Figure 3, in order to achieve the same saturation efficiency, the required air speed will decrease as the fibre length increases. For example, in order to achieve the saturation efficiency of 0.9, the incoming air velocities should be 0.29m/s, 0.16m/s, 0.10m/s and 0.08m/s respectively for the hollow fibre length of 0.208m, 0.408m, 0.608m and 0.808m.

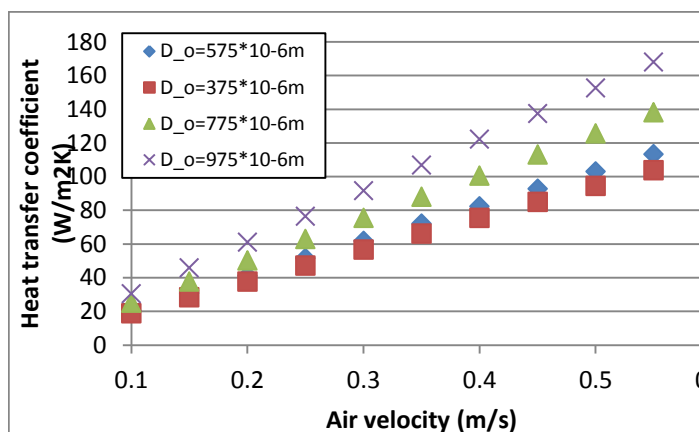### 1.2 Coefficients of heat and mass transfer

Comparison of the heat and mass transfer coefficients reveal different performance for various fibre outside diameters.

Variations of heat transfer coefficients with respect to various air velocities at different hollow fibre outside diameters (Do=375μm, 575 μm, 775 μm and 975 μm) are shown in Figure 5. It can be found that, in general, the heat transfer coefficients increase as the air velocity increases from 0.1m/s to 0.6m/s. For instance, for fibre outside diameter of 575μm, the heat transfer coefficient increases from 41.14W/m^{2}K to 102.90W/m^{2}K as the air velocity increases from 0.2m/s to 0.5m/s.

Investigations of Figure 5 further reveals that at the same air speed, the fibre with larger outside diameter will produce higher heat transfer coefficient. For example, when the air velocity is fixed at 0.4m/s, the heat transfer coefficients increases from 75.47W/m^{2}K to 82.32W/m^{2}K, 100.50W/m^{2}K till 122.09 W/m^{2}K, as the fibre outside diameter increases from 375μm to 575 μm, 775 μm until 975 μm, with percentage improvements of 9.1%, 21.5% and 22.1% respectively.

Figure 5 Variations of heat transfer coefficients with respect to various air velocities at different hollow fibre outside diameters

The variations of mass transfer coefficients with respect to various air velocities at different hollow fibre outside diameters are shown in Figure 6. Similarly to Figure 5, the mass transfer coefficients also improve as a result of the increase of air speed. For example, for fibre outside diameter of 775μm, the mass transfer coefficient increases from 2.57 W/m^{2}K to 10.28W/m^{2}K

as the air velocity increases from 0.1m/s to 0.4m/s. The increasing of the fibre outside diameter leads to the reduction of the mass transfer coefficient. For instance, at the fixed air speed of 0.5m/s, the mass transfer coefficients reduces from 26.55W/m^{2}K to 17.34W/m^{2}K, 12.84W/m^{2}K until 10.21W/m^{2}K when the fibre outside diameter increases from 375μm to 575 μm, 775 μm until 975 μm.

Figure 7 and Figure 8 shows the non-dimensional correlations of heat and mass transfer coefficients obtained with various fibre outside diameters. It would be very useful to compare the simulation obtained correlations with the experimental data, and validate the results later on.
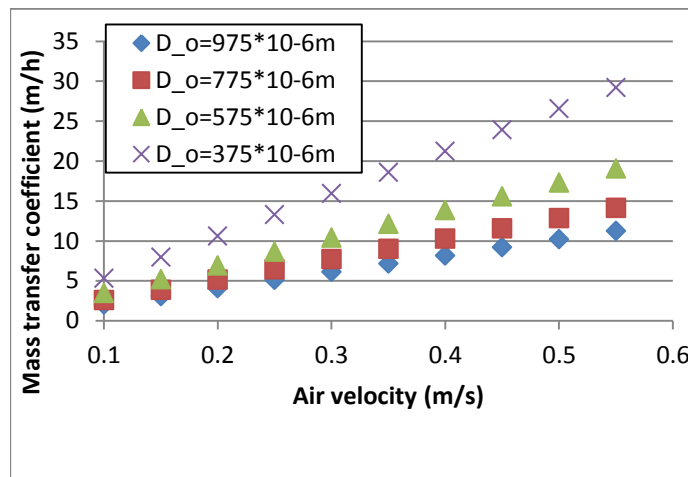

Figure 6 Variations of mass transfer coefficients with respect to various air velocities at different hollow fibre outside diameters
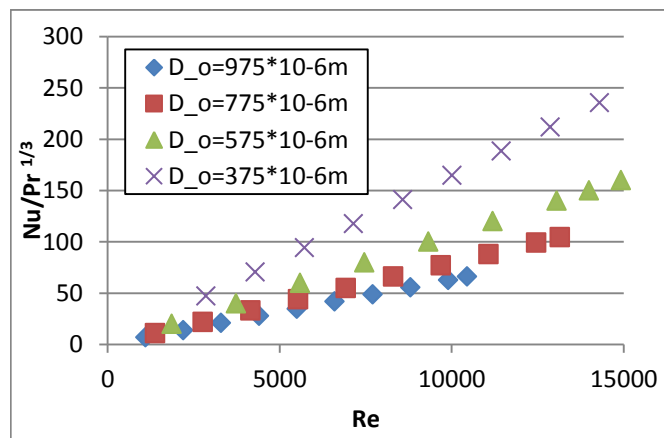

Figure 7 Non-dimensional correlations of heat transfer coefficients under various Re numbers
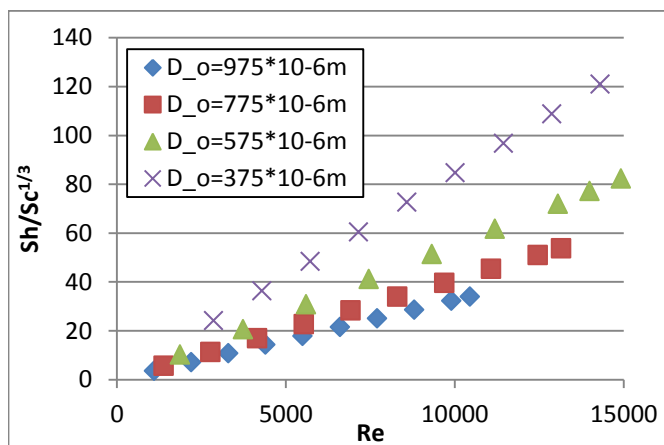
Figure 8 Non-dimensional correlations of mass transfer coefficients under various Re numbers
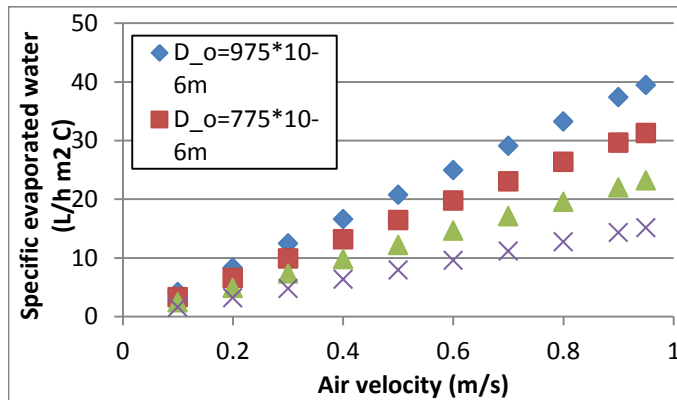
1.3 Evaporated water

Figure 9 Comparison of the specific water consumption of the hollow fibre heat exchanger at different air speed with various fibre outside diameters

Figure 9 represents the comparison of the specific water consumption of the hollow fibre heat exchanger at different air speed with various fibre outside diameters. It can be found that the increase of air speed results in large differences of the amount of water evaporated as fibre outside diameters increases from 375µm to 575 µm, 775 µm until 975 µm. For instance, for air velocity fixed at 0.6m/s, the specific evaporated water increases from 9.564L/hm^{2}C to 14.66L/hm^{2}C, 19.77L/hm^{2}C until 24.93L/hm^{2}C, with the mean improvement of 38.1%.

CONCLUSION

This paper presents the theoretical simulation of polymer hollow fibre integrated evaporative cooling system, with the purpose to provide cooling effect in hot and dry area. With the micro size diameter of the hollow fibre (OD<0.1mm), the contact surface area between the air and cooling water is significantly increased. Moreover, by varying the porosity and the fibre inside and outside diameter, the cooling effect of the evaporative system could be adjusted accordingly. Most importantly, the fibre materials are generally made from PP, PVDF or PPS, which are cheap to produce, environmental friendly, and flexible for recycle.

The following conclusions could be drawn from the simulation results:

- The saturation efficiency of the proposed system decreases as the air velocities increases from 0.2m/s to 0.8m/s. With the fibre outside diameter of 575 µm, as the air velocity reduces from 0.7m/s to 0.6m/s, the saturation efficiency increases from 0.58 to 0.65, with percentage increase of 12.1%.
- The saturation efficiency decreases as the air velocities increases from 0.2m/s to 0.5m/s. With the fibre length

of 0.408m, as the air velocity reduces from 0.25m/s to 0.15m/s, the saturation efficiency increases from 0.53 to 0.85, with percentage increase of 61.2%.

- The heat transfer coefficients increase as the air velocity increases from 0.1m/s to 0.6m/s. With fibre outside diameter of 575µm, the heat transfer coefficient increases from 41.14W/m2K to 102.90W/m2K as the air velocity increases from 0.2m/s to 0.5m/s. While the increasing of the fibre outside diameter leads to the reduction of the mass transfer coefficient.

- The increase of air speed results in large differences of the amount of water evaporated as fibre outside diameters increases from 375µm to 575 µm, 775 µm until 975 µm. With air velocity fixed at 0.6m/s, the specific evaporated water increases from 9.564L/hm2C to 14.66L/hm2C, 19.77L/hm2C until 24.93L/hm2C, with the mean improvement of 38.1%.

The simulation results demonstrated that such proposed polymer hollow fibre integrated evaporative cooling system have similar cooling effect compared with conventional evaporative cooling system with porous pad materials[4, 5]. The advantages of cheap price, flexibility of recycling, low weight for assembly and low carbon emission during the manufacturing process makes it very competitive in the world cooling market. The future work will involve the experimental testing of proposed polymer hollow fibre integrated evaporative cooling system, and the validation the theoretical modelling results with the experimental data. Differential equations considering heat and mass transfer process will be used for future modelling, and the simulation results will be compared with that published in literature.

REFERENCES
1. Watt, J.R. & Brown, W.K. Evaporative Air Conditioning Handbook, 3rd ed. Lilburn, GA: Fairmont. (1997).
2. Dai, Y.J. & Sumathy, K. Theoretical study on a cross-flow direct evaporative cooler using honeycomb paper as packing material. *Applied Thermal Engineering* **22**, 1417-1430 (2002).
3. Farmahini-Farahani, M., Delfani, S. & Esmaeelian, J. Exergy analysis of evaporative cooling to select the optimum system in diverse climates. *Energy* **40**, 250-257 (2012).
4. Liao, C.-M. & Chiu, K.-H. Wind tunnel modeling the system performance of alternative evaporative cooling pads in Taiwan region. *Building and Environment* **37**, 177-187 (2002).
5. Rawangkul, R., Khedari, J., Hirunlabh, J. & Zeghmati, B. Performance analysis of a new sustainable evaporative cooling pad made from coconut coir. *International Journal of Sustainable Engineering* **1**, 117-131 (2008).

6. He, S. et al. Experimental study of film media used for evaporative pre-cooling of air. *Energy Conversion and Management* **87**, 874-884 (2014).

7. Mujahid Rafique, M., Gandhidasan, P., Rehman, S. & Al-Hadhrami, L.M. A review on desiccant based evaporative cooling systems. *Renewable and Sustainable Energy Reviews* **45**, 145-159 (2015).

8. Riangvilaikul, B. & Kumar, S. An experimental study of a novel dew point evaporative cooling system. *Energy and Buildings* **42**, 637-644 (2010).

9. Caliskan, H., Hepbasli, A., Dincer, I. & Maisotsenko, V. Thermodynamic performance assessment of a novel air cooling cycle: Maisotsenko cycle. *International Journal of Refrigeration* **34**, 980-990 (2011).

10. Zhao, X., Li, J.M. & Riffat, S.B. Numerical study of a novel counter-flow heat and mass exchanger for dew point evaporative cooling. *Applied Thermal Engineering* **28**, 1942-1951 (2008).

11. Zhao, X., Yang, S., Duan, Z. & Riffat, S.B. Feasibility study of a novel dew point air conditioning system for China building application. *Building and Environment* **44**, 1990-1999 (2009).

12. standards, A. Heating, ventilating and cooling greenhouses, American Society of Agricultural and Biological Engineers, St. Joseph, Michigan, USA, . (2008).

13. Franco, A., Valera, D.L., Madueño, A. & Peña, A. Influence of water and air flow on the performance of cellulose evaporative cooling pads used in mediterranean greenhouses. *Transactions of the ASABE* **53**, 565-576 (2010).

14. Dowdy, J.A., Reid, R.L. & Handy, E.T. in ASHRAE Transactions 60-70 (1986).